



Exploring the fatty acids of *vernix caseosa* in form of their methyl esters by off-line coupling of non-aqueous reversed phase high performance liquid chromatography and gas chromatography coupled to mass spectrometry

Simone Hauff, Walter Vetter*

University of Hohenheim, Institute of Food Chemistry, Garbenstrasse 28, D-70599 Stuttgart, Germany

ARTICLE INFO

Article history:

Received 9 July 2010

Received in revised form

29 September 2010

Accepted 25 October 2010

Available online 30 October 2010

Keywords:

Vernix caseosa

Fatty acid methyl esters

Branched chain fatty acids

Non-aqueous reversed phase HPLC

GC/EI-MS

Two dimensional contour plot

Enantioseparation

ABSTRACT

Vernix caseosa is a greasy biofilm formed on the skin of the human fetus in the last period of pregnancy. This matrix is known to contain a range of uncommon branched chain fatty acids. In this study, we studied the fatty acid composition of vernix caseosa by non-aqueous reversed phase high performance liquid chromatography (RP-HPLC) fractionation followed by gas chromatography–electron ionization mass spectrometry (GC/EI-MS) of the fractions. For this purpose the fatty acids from vernix caseosa were converted into the corresponding methyl esters. These were fractionated by non-aqueous RP-HPLC using three serially connected C_{18} -columns and pure methanol as the eluent. Aliquots of the HPLC fractions were directly analyzed by GC/EI-MS in the selected ion monitoring mode. Data analysis and visualization were performed by the creation of a two dimensional (2D) contour plot, in which GC retention times were plotted against the HPLC fractions. Inspection of the plot resulted in the detection of 133 different fatty acids but only 16 of them contributed more than 1% to the total fatty acids detected. Identification was based on HPLC and GC retention data, GC/MS-SIM and full scan data, as well as plotting the logarithmic retention times against the longest straight carbon chain. In selected cases, aliquots of the HPLC fractions were hydrogenated or studied by means of the picolinyl esters. Using these techniques, the number of double bonds could be unequivocally assigned to all fatty acids. Moreover, the number of methyl branches, and in many cases the positions of methyl branches could be determined. The enantioselective analysis of chiral anteiso-fatty acids resulted in the dominance of the *S*-enantiomers. However, high proportions of *R*-a13:0, *R*-a15:0, and *R*-a17:1 were also detected while a17:0 was virtually *S*-enantiopure.

© 2010 Elsevier B.V. All rights reserved.

1. Introduction

Vernix caseosa is a white, greasy biofilm which covers and protects the skin of the human fetus in the last period of pregnancy [1]. It is still frequently present after birth [1]. Structurally, it is composed of corneocytes surrounded by ~10% lipids [1,2]. Lipids play a major role in the protective properties of vernix caseosa [2]. Remarkably, the fatty acids in vernix caseosa differ much from those found in food and most other biological samples. The most relevant fatty acids described in vernix caseosa were reported to be straight and methyl-branched fatty acids along with monoenoic fatty acids [3,4]. Due to the protective properties, the unusual fatty acids of vernix caseosa may be very valuable and their biochemistry needs to be explored in detail. However, most fatty acids in

this matrix are not available as reference standards and the peak assignment is not trivial. Hence, the use of mass spectrometry for determination of the fatty acids as methyl esters (FAMES) is virtually essential.

Unfortunately, mass spectra of FAMES are frequently equivocal and in view of the fact that many FAs are not available as standards, the structure assignment to a peak detected by GC is not straight forward. A drawback is that the methods previously used for fatty acid analysis of vernix caseosa are either very complex (i.e. combination of many different techniques for fractionation [5]) or incomplete (only a limited number of fatty acids were determined [3,6]). It was assumable that analysis of such complex mixtures may benefit from the analysis by ample two dimensional techniques. For instance, the merits of comprehensive gas chromatography ($GC \times GC$) in the field of lipid analysis have been repeatedly explored [7–13]. Recently, we fractionated fish oil by non-aqueous reversed phase (RP-) HPLC fractionation followed by gas chromatography coupled to electron ionization mass spectrometry selected ion monitoring (GC/EI-MS-SIM) analysis [14]. In order to visualize structural features, a comprehensive 2D plotting of the

* Corresponding author at: University of Hohenheim, Institute of Food Chemistry (170b), Garbenstrasse 28, D-70599 Stuttgart, Germany. Tel.: +49 711 459 24016; fax: +49 711 4594377.

E-mail address: w-vetter@uni-hohenheim.de (W. Vetter).

GC separated HPLC fractions was facilitated by the creation of a 2D-contour plot [15]. This method allowed determining the various fatty acids in fish oil virtually without co-elution. In this study, we used this off-line RP-HPLC and GC/EI-MS technique to determine the fatty acids of vernix caseosa after conversion into the corresponding methyl esters. In addition, samples of vernix caseosa are known to contain a number of chiral fatty acids including *anteiso*-fatty acids which can be resolved by application of modified cyclodextrins [16–18]. The HPLC method was also found suitable to gather fractions simple enough for the direct enantioselective analysis by GC/EI-MS [17]. Thus, left-overs from the GC/EI-MS analysis of RP-HPLC fractions were used to study the enantioseparation of *anteiso*-fatty acids.

2. Materials and methods

2.1. Chemicals, standards and samples

The solvents methanol, *n*-hexane, tetrahydrofuran (THF) (all HPLC gradient grade), as well as ethanolic BF₃ (~10%) solution were ordered from Fluka (Taufkirchen, Germany). Methanolic BF₃ (~13%) and PtO₂ (Adam's catalyst) were from Riedel-de-Haën (Taufkirchen, Germany) and *iso*-octane (for GC analyses) was purchased from Merck (Darmstadt, Germany). Hydrogen (purity 99.9990%) was from Sauerstoffwerke (Friedrichshafen, Germany). FAMES from standards and sample were prepared using the boron trifluoride method as recently reported [19]. A bulk sample of vernix caseosa sample was collected in a hospital close to Stuttgart, Germany. The initial sample concentration was 20 mg/mL. Five percent of this solution (50 µL = 1 mg) was injected via a Rheodyne 7010 injector fitted with a 100 µL loop. The fractions were collected at time intervals of 0.5 min. Then, 10 µL (1 µg) of the internal standard solution undecanoic acid ethyl ester (11:0 EE) was added to sample and standard solutions prior to GC/MS injection in order to adjust time shifts and variations in the peak high intensities from injection to injection [19].

2.2. Non-aqueous reversed phase high performance liquid chromatography (RP-HPLC) fractionation

Non-aqueous RP-HPLC fractionation of FAMES was performed according to Hauff and Vetter [19]. In brief, a Varian solvent pump and a Varian ProStar 325 UV-Vis detector (dual wavelength mode using 206 nm and 234 nm) followed by an evaporative light scattering detector (ELSD) (PLELS 2100, Polymer Laboratories). Separations were performed at room temperature by means of three 4.6 mm i.d. C₁₈ columns connected to a total length of 75 cm [19]. Methanol was used as mobile phase, with a flow rate at 0.9 mL/min. HPLC fractions were collected every 0.5 min and aliquots were directly/after dilution subjected to GC/EI-MS analysis [19].

2.3. Non-chiral gas chromatography in combination with electron ionization mass spectrometry (GC/EI-MS)

Analyses were performed with an HP 5890 gas chromatograph coupled to an HP 5971 mass selective detector (Hewlett-Packard, Waldbronn, Germany) as recently described [20] with the following modifications: A 60 m × 0.25 mm i.d. fused silica capillary column coated with 0.1 µm 90% biscyanopropyl-10% phenylcyanopropyl polysiloxane (Rtx-2330, Restek Bellefonte, USA) was installed in the GC oven. The GC oven was held for 2 min at 55 °C, then the temperature was ramped with 10 °C/min at 170 °C and thereafter with 3 °C/min at 250 °C, which was held for 10 min (the total run time was 50.17 min). The carrier gas helium 5.0 (Sauerstoffwerke, Friedrichshafen) was transported with a constant flow

rate at 1.0 mL/min through the column. For GC/EI-MS measurements a solvent delay of 8 min was applied. In the SIM mode we recorded the six fragment ions *m/z* 74 and *m/z* 87 for saturated and monounsaturated FAMES, *m/z* 81 and *m/z* 79 for dienoic and polyenoic FAMES [21], and *m/z* 88 and *m/z* 101 for the IS 11:0 EE throughout the run [19]. The latter two ions also served for the determination of 2-methyl-branched FAMES (*m/z* 101 corresponds the β-cleavage of this FA with an additional β-methyl group) [22].

In the GC/EI-MS full scan mode, two methods were used to determine the molecular ion and to locate the position of the methyl groups. A smaller scan range (*m/z* 200–450; 2.7 scans per second) supports the detection of the molecular ion. This technique was used for analysis of HPLC fractions 30–40. These contained many different FAMES which could not be determined without M⁺. Other fractions contained fatty acids with important fragment ions in the range below 200 u. These were targeted with the wider full scan range (*m/z* 50–450; 1.8 scans per second). A methyl branch in 2-position is characterized by particular abundance of *m/z* 88 (instead of *m/z* 74), whereas 6-methyl- and 8-methyl branches are characterized by abundant [M-76]⁺ ions and *m/z* 143, respectively [23,24].

2.4. Enantioselective gas chromatography in combination with electron ionization mass spectrometry (GC/EI-MS)

Enantioselective measurements were performed with an HP GCD plus system equipped with an HP 6890 autosampler (Hewlett-Packard, Waldbronn, Germany) using parameters described elsewhere in detail [18]. For GC/EI-MS-SIM mode, nine fragment ions (*m/z* 74, *m/z* 87, *m/z* 81, and *m/z* 79 for all FAMES along with five specific ones, i.e. *m/z* 284 (M⁺ for 17:0 ME isomers), *m/z* 256 (M⁺ for 15:0 ME isomers), *m/z* 282 (M⁺ for 17:1 ME isomers), *m/z* 250 ([M-32]⁺ for 17:1 ME isomers), and *m/z* 208 ([M-74]⁺ for 17:1 ME isomers) were recorded throughout the run. A solvent delay of 100 min was applied. A 30 m × 0.25 mm i.d. column coated with 50% heptakis(6-*O*-*tert*-butyldimethylsilyl)-2,3-di-*O*-methyl)-β-cyclodextrin (β-TBDM) in OV-1701 prepared according to Dietrich et al. [25] was installed in the GC oven [18]. The GC oven program was as follows: After 1 min at 60 °C, the temperature was ramped at 10 °C/min to 115 °C (hold time 400 min), and finally ramped at 1 °C/min to 137 °C (hold time 221 min).

2.5. Hydrogenation of unsaturated fatty acids [26]

Suitable HPLC fractions were evaporated to dryness and re-dissolved in ~2 mL dry THF. This solution plus 2 mg PtO₂ was stirred in an H₂ atmosphere maintained with an H₂-filled balloon attached to the flask [18]. After 1 h reaction time, the resulting saturated FAMES were filtered through celite 545 to remove the catalyst, before the THF was evaporated and replaced by *iso*-octane for following GC/EI-MS measurements [18].

2.6. Picolinyl esters of fatty acids

Aliquots of the HPLC fractions were evaporated and re-dissolved in 1 mL dry CH₂Cl₂. Potassium *tert*-butoxide in THF (20%, 0.1 mL) and 3-hydroxymethylpyridine (0.2 mL) was added and the solution was mixed and kept for 30 min at 40 °C. After cooling to room temperature 2 mL saturated NaCl solution was added and the picolinyl esters were extracted three times with 2 mL *n*-hexane. The volume of the *n*-hexane phase was adjusted to 1 mL and analyzed by GC/EI-MS [27–29].

2.7. Data analysis

Data analysis was performed as recently described by Kapp and Vetter [15] in the modified mode of Hauff and Vetter [14]. To

Table 1
Structures, longest straight chain, GC (t_R , $\log t_R$) and HPLC information, contribution to the total fatty acids and identification information for 133 fatty acids detected in vernix caseosa.

No.	Structure	Longest straight chain	$\log t_R$ (GC)	GC t_R (min)	HPLC fraction	% of total fatty acids	SIM ion characteristics	Identified/tentatively identified (TI)
Saturated fatty acids								
1	12:0	12	114.8	14.07	26	0.27	74 > 87	Standard
2	i13:0 (11-Me-12:0)	12	115.8	14.38	26	0.04	74 > 87	TI by RRT, 2D & $\log t_R$ plot
3	Me-12:0	12	115.9	14.43	26	0.32	87 > 74	TI by $\log t_R$ plot
4	Me-12:0	12	116.4	14.57	26	0.01	74 > 87	TI by $\log t_R$ plot
5	a13:0 (10-Me-12:0)	12	116.8	14.72	26	0.34	74 > 87	Standard
6	diMe-12:0	12	116.9	14.76	26	0.19	87 > 74	TI by $\log t_R$ plot
7	diMe-12:0	12	117.5	14.96	26	0.03	74 > 87	TI by $\log t_R$ plot
8	13:0	13	117.6	15.00	30	0.02	74 > 87	Standard
9	Me-13:0	13	118.4	15.29	30	0.02	74 > 87	TI by $\log t_R$ plot
10	Me-13:0	13	118.6	15.35	30	0.18	87 > 74	4-Me-13:0, RRT
11	i14:0 (12-Me-13:0)	13	119.1	15.51	30	4.19	74 > 87	Standard
12	Me-13:0	13	119.4	15.63	30	0.07	87 > 74	M^+ , m/z 256
13	6,x-diMe-13:0	13	119.8	15.79	30	0.12	74 > 87	M^+ , m/z 256, TI by RRT and m/z 180 = [M-76] ⁺
14	4,x-diMe-13:0	13	120.0	15.86	30	0.21	87 > 74	M^+ , m/z 256, TI by RRT and fragmentation
15	2,x-diMe-13:0	13	120.4	16.01	32	0.04	88 > 101	TI by $\log t_R$ plot
16	6,x-diMe-13:0	13	121.1	16.27	31	1.37	74 > 87	M^+ , m/z 256, M-76 = m/z 180, $\log t_R$ plot, same substitution as no. 31 & 48
17	4,11-diMe-13:0	13	121.2	16.30	32	4.08	87 > 74	TI by RRT, M^+ , MS and literature [31]
18	8,x-diMe-13:0	13	121.4	16.35	31	1.52	74 > 87	M^+ , m/z 256, m/z 143
19	4,8,12-triMe-13:0	13	121.9	16.55	32	0.35	87 > 74	M^+ , m/z 270, TI by RRT, M^+ , MS, and literature [22]
20	triMe-13:0	13	122.5	16.79	32	0.06	74 > 87	M^+ , m/z 270
21	2-Me-14:0	14	119.8	15.78	33	0.16	88 > 101	M^+ , m/z 256, TI by HPLC fraction, MS
22	14:0	14	120.3	15.97	34	16.99	74 > 87	Standard
23	Me-14:0	14	121.4	16.37	35	0.00	88 > 101	TI by $\log t_R$ plot
24	Me-14:0	14	121.5	16.41	35	0.01	74 > 87	M^+ , m/z 256
25	Me-14:0	14	121.6	16.44	33	0.05	88 > 101	TI by $\log t_R$ plot
26	i15:0 (13-Me-14:0)	14	121.6	16.46	35	1.36	74 > 87	Standard
27	a15:0 (12-Me-14:0)	14	122.1	16.63	34	4.03	74 > 87	Standard
28	4,x-diMe-14:0	14	122.6	16.82	33	0.17	87 > 74	M^+ , m/z 270
29	8,x-diMe-14:0	14	123.6	17.22	34	0.99	74 > 87	M^+ , m/z 270, most likely 6,8-diMe-14:0; co-elution with no. 30 (HPLC separated)
30	6,x-diMe-14:0	14	123.7	17.24	35	0.08	74 > 87	M^+ , m/z 270, m/z 194 (M-76)
31	diMe-14:0	14	123.7	17.28	34	0.61	74 > 87	M^+ , m/z 270, TI by $\log t_R$ plot, most likely same substitution as no. 16 & 48
32	4,12-diMe-14:0	14	123.8	17.29	37	1.97	87 > 74	TI by RRT, M^+ and MS [31]
33	diMe-14:0	14	124.1	17.43	36	0.69	74 > 87	M^+ , m/z 270, TI by $\log t_R$ plot
34	triMe-14:0	14	124.4	17.53	35	0.09	87 > 74	TI by $\log t_R$ plot
35	4,8,12-triMe-14:0	14	124.6	17.63	35	0.04	87 > 74	M^+ , m/z 284, TI by RRT and MS
36	2-Me-15:0	15:0	122.4	16.74	38	0.50	88 > 101	M^+ , m/z 270, TI by HPLC fraction and MS
37	15:0	15	122.9	16.93	39	10.38	74 > 87	Standard
38	2-Me-X	15	123.0	16.97	37	0.01	88 > 101	TI by $\log t_R$ plot
39	2-Me-X	15	123.6	17.21	39	0.01	88 > 101	TI by $\log t_R$ plot
40	2-Me-X	15	124.0	17.37	41	0.00	88 > 101	TI by $\log t_R$ plot
41	i16:0	15	124.2	17.47	41	0.25	74 > 87	Standard
42	Me-15:0	15	125.2	17.85	37	0.30	74 > 87	M^+ , m/z 284

Table 1(Continued)

No.	Structure	Longest straight chain	log t_{R} (GC)	GC t_{R} (min)	HPLC fraction	% of total fatty acids	SIM ion characteristics	Identified/tentatively identified (TI)
43	Me-15:0	15	125.2	17.86	38	0.15	87 > 74	TI by log t_{R} plot
44	4-Me,x-diMe-15:0	15	125.7	18.09	38	0.01	87 > 74	M^+ , m/z 284, with one of the two methyl branches on C4
45	2-Me,x-diMe-15:0	15	126.0	18.21	42	0.00	88 > 101	TI by log t_{R} plot
46	6,x-diMe-15:0	15	126.2	18.27	39	0.01	74 > 87	M^+ , m/z 284, (M-76); 6,8-diMe and/or coelution of 6,x-diMe and 8,x-diMe (see no. 29/30)
47	4,11-diMe-15:0	15	126.4	18.36	43	0.33	87 > 74	TI by RRT, M^+ , MS [31]
48	diMe-15:0	15	126.5	18.42	41	0.14	74 > 87	TI by log t_{R} plot, most likely same substitution as no. 16 and no. 31
49	diMe-15:0	15	126.9	18.59	41	0.00	87 > 74	TI by log t_{R} plot
50	triMe-15:0	15	127.2	18.69	41	0.00	87 > 74	TI by log t_{R} plot
51	triMe-15:0	15	127.4	18.81	41	0.01	87 > 74	TI by log t_{R} plot
52	triMe-15:0	15	128.0	19.04	41	0.01	74 > 87	TI by log t_{R} plot
53	2-Me-16:0	16	125.0	17.75	45	1.31	88 > 101	M^+ , m/z 284, TI by HPLC fraction, MS
54	16:0	16	125.5	18.00	47	13.59	74 > 87	Standard
55	Me-16:0	16	126.6	18.45	51	0.01	74 > 87	TI by log t_{R} plot
56	i17:0 (15-Me-16:0)	16	126.8	18.55	47	0.04	74 > 87	Standard
57	a17:0 (14-Me-16:0)	16	127.3	18.74	45	0.90	74 > 87	Standard
58	diMe-16:0	16	127.8	18.97	44	0.01	87 > 74	TI by log t_{R} plot
59	diMe-16:0	16	128.0	19.08	51	0.02	74 > 87	TI by log t_{R} plot
60	diMe-16:0	16	128.2	19.15	43	0.17	87 > 74	TI by log t_{R} plot
61	diMe-16:0	16	128.3	19.21	44	0.02	87 > 74	TI by log t_{R} plot
62	diMe-16:0	16	128.8	19.39	46	0.03	74 > 87	TI by log t_{R} plot
63	6,x-diMe-16:0	16	128.8	19.42	45	0.04	74 > 87	TI by log t_{R} plot; most likely 6,8-diMe and coelution (see no. 29/30 and 46)
64	diMe-16:0	16	129.0	19.49	45	0.06	74 > 87	TI by log t_{R} plot
65	4,x-diMe-16:0	16	129.0	19.50	50	0.18	87 > 74	TI by log t_{R} plot, with $x = 11$ or 12
66	17:0	17	128.0	19.06	59	2.85	74 > 87	Standard
67	i18:0 (16-Me-17:0)	17	129.5	19.71	60	0.17	74 > 87	Standard
68	18:0	18	130.7	20.29	72	1.85	74 > 87	Standard
Monoenoic fatty acids								
69	14:1	14	121.1	16.25	26	0.05	74 > 87 > 79/81	TI by RRT, MS
70	14:1	14	121.2	16.29	26	0.04	74 > 87 > 79/81	TI by RRT, MS
71	14:1	14	121.5	16.42	26	0.72	74 > 87 > 79/81	TI by RRT, MS
72	14:1(9)	14	121.9	16.58	26	0.03	74 > 87 > 79/81	Standard
73	14:1	14	122.1	16.65	26	0.03	74 > 87 > 79/81	TI by RRT, MS
74	14:1	14	122.3	16.72	26	0.02	74 > 87 > 79/81	TI by RRT, MS
75	Me-14:1	14	122.8	16.91	26	0.29	74 > 87 > 79/81	TI, double bond position [34][35];
76	15:1tr	15	123.8	17.28	30	0.04	74 > 87 > 79/81	TI by late elution from HPLC
77	15:1	15	124.1	17.40	27	0.57	74 > 87 > 79/81	TI by RRT, MS
78	15:1(10)	15	124.6	17.61	27	0.00	74 > 87 > 79/81	Standard
79	Me-15:1	15	124.9	17.76	29	0.01	74 > 87 > 79/81	i16:1(9) or 16:1(8)
80	i16:1(6)	15	125.4	17.94	29	0.40	74 > 87 > 79/81	TI by RRT, MS, literature [31], double bond position [34]
81	16:1	16	126.3	18.33	33	0.40	74 > 87 > 79/81	TI by RRT, MS
82	16:1	16	126.6	18.45	29	0.11	74 > 87 > 79/81	TI by RRT, MS
83	16:1(9)	16	126.8	18.55	30	9.46	74 > 87 > 79/81	Standard
84	16:1	16	127.0	18.61	30	1.38	74 > 87 > 79/81	TI by RRT, MS
85	16:1	16	127.3	18.73	31	0.30	74 > 87 > 79/81	TI by RRT, MS
86	16:1	16	127.4	18.81	31	0.15	74 > 87 > 79/81	TI by RRT, MS
87	i17:1	16	128.0	19.04	32	0.11	74 > 87 > 79/81	TI by RRT and MS
88	a17:1(6)	16	128.5	19.26	31	0.99	74 > 87 > 79/81	TI by hydrogenation, RRT and double bond position [34]

Table 1(Continued)

No.	Structure	Longest straight chain	log t_R (GC)	GC t_R (min)	HPLC fraction	% of total fatty acids	SIM ion characteristics	Identified/tentatively identified (TI)
89	17:1tr?	17	128.9	19.47	37	0.04	74 > 87 > 79/81	TI by RRT, MS
90	17:1(6)	17	129.3	19.65	33	1.56	74 > 87 > 79/81	Identified as picolinyl ester
91	17:1	17	129.4	19.68	32	0.04	74 > 87 > 79/81	TI by RRT, MS
92	17:1	17	129.7	19.82	33	0.16	74 > 87 > 79/81	TI by RRT, MS
93	17:1	17	130.5	20.20	34	0.04	74 > 87 > 79/81	TI by RRT, MS
94	Me-17:1	17	130.1	19.99	35	0.01	74 > 87 > 79/81	i18:1(6), TI by RRT, MS and double bond [34]
95	Me-17:1	17	130.6	20.25	35	0.10	74 > 87 > 79/81	i18:1(8), TI by RRT, MS, and double bond position [34]
96	18:1(9tr)	18	131.7	20.75	37	0.01	74 > 87 > 79/81	Standard
97	18:1(8)	18	132.0	20.91	37	3.23	74 > 87 > 79/81	Identified as picolinyl ester
98	18:1	18	132.1	20.95	37	2.07	74 > 87 > 79/81	TI by RRT, MS
99	18:1	18	132.3	21.02	39	0.12	74 > 87 > 79/81	TI by RRT, MS
100	18:1	18	132.6	21.19	39	0.06	74 > 87 > 79/81	TI by RRT, MS
101	18:1	18	133.0	21.36	38	0.02	74 > 87 > 79/81	TI by RRT, MS
102	19:1	19	134.6	22.18	42	0.05	74 > 87 > 79/81	TI by RRT, MS
103	19:1	19	134.7	22.24	42	0.05	74 > 87 > 79/81	TI by RRT, MS
104	20:1	20	137.3	23.58	50	0.03	74 > 87 > 79/81	TI by RRT, MS
105	20:1(10)	20	137.3	23.62	50	0.03	74 > 87 > 79/81	TI by RRT, MS
106	20:1	20	137.7	23.82	50	0.05	74 > 87 > 79/81	TI by RRT, MS
Dienoic fatty acids								
107	16:2	16	127.8	18.98	26	0.01	81 > 79	TI by RRT, MS
108	16:2	16	128.1	19.11	26	0.01	81 > 79	TI by RRT, MS
109	16:2	16	128.3	19.20	26	0.01	81 > 79	TI by RRT, MS
110	16:2	16	128.4	19.25	26	0.02	81 > 79	TI by RRT, MS
111	16:2	16	128.8	19.39	26	0.05	81 > 79	TI by RRT, MS
112	16:2	16	128.9	19.47	26	0.26	81 > 79	TI by RRT, MS
113	16:2	16	129.8	19.85	26	0.08	81 > 79	TI by RRT, MS
114	17:2	17	131.4	20.59	28	0.02	81 > 79	TI by RRT, MS, and log t_R plot
115	17:2	17	131.5	20.68	28	0.02	81 > 79	TI by RRT, MS, and log t_R plot
116	18:2	18	132.0	20.89	32	0.16	81 > 79	TI by RRT, MS
117	18:2	18	133.1	21.44	30	0.01	81 > 79	TI by RRT, MS
118	18:2 (9,12)	18	133.4	21.56	30	0.05	81 > 79	Standard
119	18:2	18	133.6	21.67	31	0.07	81 > 79	TI by RRT, MS
120	18:2	18	133.9	21.81	31	0.58	81 > 79	TI by RRT, MS
121	18:2 (12,15)	18	134.1	21.94	30	0.16	81 > 79	Standard
122	18:2	18	134.3	22.05	31	0.24	81 > 79	TI by RRT, MS
123	18:2	18	135.2	22.49	31	0.05	81 > 79	TI by RRT, MS
124	18:2	18	135.3	22.54	30	0.17	81 > 79	TI by RRT, MS
125	20:2	20	138.8	24.45	39	0.22	81 > 79	TI by RRT, MS
126	20:2	20	138.9	24.51	38	0.06	81 > 79	TI by RRT, MS
127	20:2 (11,14)	20	139.3	24.70	38	0.04	81 > 79	Standard
Trienoic fatty acids								
128	18:3 isomer	18	134.9	22.34	27	0.02	79 > 81	TI by RRT, MS
129	18:3 (6,9,12)	18	135.6	22.68	27	0.06	79 > 81	Standard
130	20:3	20	140.5	25.39	32	0.02	79 > 81	TI by RRT, MS
131	20:3	20	140.6	25.48	32	0.04	79 > 81	TI by RRT, MS
132	20:3(8,11,14)	20	140.9	25.63	32	0.02	79 > 81	Standard
133	20:3(11,14,17)	20	141.9	26.24	29	0.02	79 > 81	Standard
				Contribution of saturated fatty acids				
				Contribution of monoenoic fatty acids	21.6%			
				Contribution of dienoic fatty acids	2.3%			
				Contribution of trienoic fatty acids	0.2%			

facilitate the comparison of signal intensities between the different HPLC fractions, data points of each fraction were normalized to the signal intensity of the IS by dividing the signal intensity of each data point by the data point representing the peak maximum of the respective internal standard peak. Thereafter, uneven responses of different classes of fatty acids in GC/EI-MS-SIM chro-

matograms were taken into account before the 2D-contour plot was created [14]. Start and end points of each peak were determined by the automatic integration feature embedded in the MS Data Analysis software. Data resulting in a two dimensional assembly where finally arranged in a 2D-contour plot (SigmaPlot 2001, Systat Software, Erkrath, Germany), in which the HPLC fraction

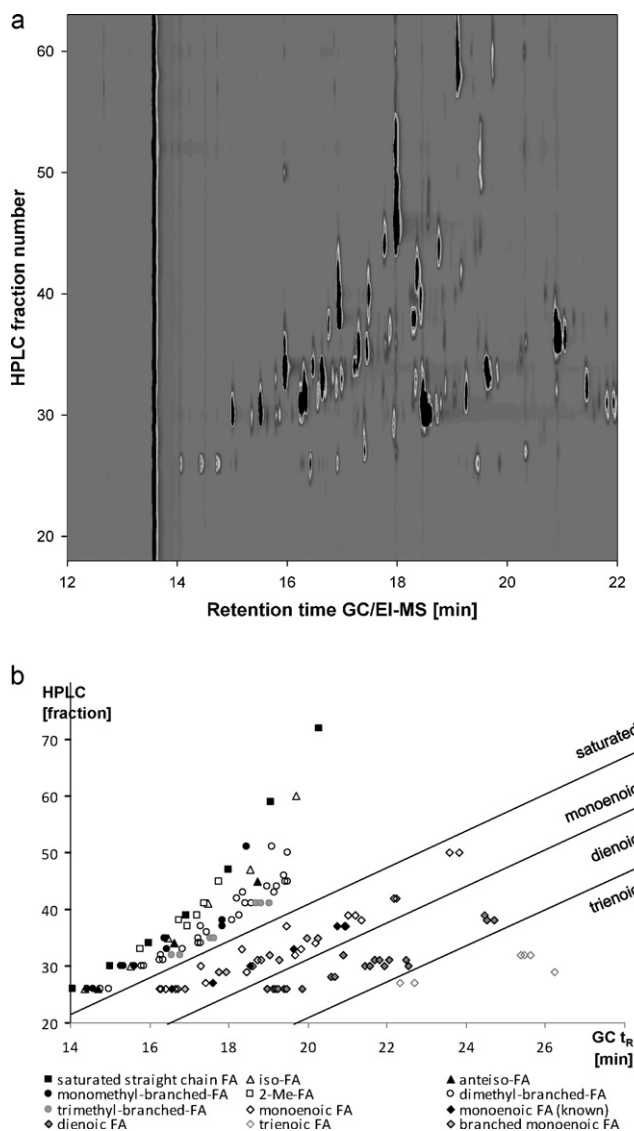


Fig. 1. (a) 2D-contour plot of the methyl esters of the fatty acids from vernix caseosa obtained by plotting the GC/EI-MS retention time against the HPLC fraction number. The sizes of the peaks reflect the relative amounts present. The vertical line ~ 13.6 min originates from the internal standard added to the HPLC fractions in order to determine relative contributions of individual fatty acids to the total fatty acids. (b) x,y-coordinate plot of the fatty acids in vernix caseosa.

number (ordinate) was plotted versus the GC/EI-MS retention time (abscissa). The spot intensities reflect the quantitative amounts of individual FAMES in relation to the IS. Fatty acids were determined as methyl esters, but in the following, they will be presented and discussed as fatty acids only, for reasons of simplicity.

3. Results and discussion

3.1. General characteristics of the 2D plot

The basic retention properties of FAMES in RP-HPLC [30–32] are complementary to those obtained by GC/EI-MS on a polar stationary phase [14]. Thus, the fatty acids were widely distributed in the 2D plot (Fig. 1a). RP-HPLC and GC/EI-MS retention times of saturated fatty acids both increased with the carbon chain length. However, unsaturated fatty acids with the same chain length eluted the faster from the HPLC system the more double bonds they contained whereas this was reversed in GC/EI-MS. As a consequence,

the saturated, the monoenoic, and the polyenoic fatty acids were grouped in separated areas in the 2D-plot (Fig. 1b). For this reason, the number of double bonds in a fatty acid could directly be derived from its position in the 2D plot. GC/EI-MS-SIM measurements (see Section 2.3) confirmed that all detected compounds were fatty acids and not alcohols which had been assumed to be present in vernix caseosa [3]. A thorough inspection of the 2D-plot led to the detection of 133 fatty acids (68 saturated, 38 monoenoic, 21 dienoic and six trienoic fatty acids with carbon numbers ranging from C_{12} to C_{20} , Table 1). Since a double bond equals with about two carbons in RP-HPLC, saturated FAMES with longest straight chain of C_{12} were on the same horizontal level as 14:1, 16:2 and 18:3 isomers. In order to better visualize the structural relationship of the fatty acids detected as well as the regions of fatty acids classes in the 2D-plot we created an x,y-coordinate plot (Fig. 1b).

3.2. Saturated fatty acids in vernix caseosa

Seven straight chain, six *iso*-branched and three *anteiso*-branched homologues were identified by means of authentic reference standards (Table 1). Hence the remaining ~ 50 fatty acids in this group were mono- and multibranch saturated FAMES. In agreement with fish samples and dairy products, *iso*-fatty acids were detected from i13:0 through i18:0 whereas only odd-numbered *anteiso*-FAs were detected (Table 1). Branched chain fatty acids are candidates for agents that play a role in gut colonization and have been proposed to be a nutritional component for the fetus/newborn [33]. When GC/EI-MS was used in the full scan mode, the molecular ion could not be detected for all FAMES because of the low abundance of individual FAMES. The complete or partial structure assignment of fatty acids was based on HPLC fraction, GC retention times, and fragment ions in GC/EI-MS-SIM and scan modes. Since the HPLC elution was related to the longest chain in the molecule, a C_{16} fatty acid (M^+ , m/z 270) eluted in the “ C_{15} HPLC fraction” if monomethyl-branched, in the “ C_{14} HPLC fraction” if dimethyl-branched and in the “ C_{13} HPLC fraction” if trimethyl-branched. For this reason, the saturated fatty acids were listed with regard to the longest straight chain in the molecules (Table 1).

Mass spectra of FAMES with a methyl branch on C-2 show the McLafferty ion shifted to m/z 88 along with m/z 101 [22]. This feature was found on ten fatty acids (Table 1). Three of them could be traced back to 2-Me-14:0, 2-Me-15:0, and 2-Me-16:0. In total, seven saturated FAMES with 12 carbons in the longest chain were detected. The shortest retention time was found for 12:0 (because it contains one carbon less) while i13:0 and a13:0 marked retention time #2 and #5 in this group of C_{12} being the longest carbon chain. In agreement with previous measurements of isostearates [29], the *anteiso*-congener was the last eluting monomethyl-branched homolog (Table 1). We also took advantage of plotting the logarithms of the GC retention times ($\log t_R$) against the length of the longest chain [3][34]. As can be seen from this plot, fatty acids with the same substitution but different chain length (e.g. straight chain, *iso*-, and *anteiso*-fatty acids) were located on straight parallel lines (Fig. 2). Consequently, the line through the *anteiso*-fatty acids marked the border between monomethyl- and dimethyl-substituted fatty acids which shared the same longest carbon chain (Fig. 2).

Two isomers in the group with twelve carbons in the longest chain showed a higher abundance of m/z 87 compared to m/z 74. This feature was reported to be typical for 4-methyl substituted isomers. Most likely, the first eluting one was 4-Me-12:0 while the nature of the second one with this feature and the two other isomers remained unknown. Thirteen isomers with C_{13} as longest carbon chain were detected which eluted into HPLC fraction 30–32. In this pool, we were able to assign 13:0 along with four mono-, six di- and two trimethyl-branched homologues. A similar pattern was

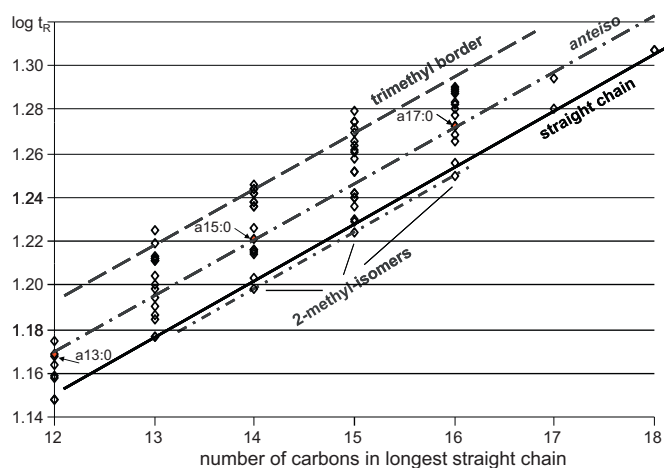


Fig. 2. Plot of logarithmic retention times ($\log t_R$) against the length of the longest carbon chain of saturated straight chain and branched chain fatty acids in vernix caseosa.

observed for homologues with C_{14} as the longest chain. In this group the first eluted congener was identified as 2-Me-14:0. This type of fatty acid was also the first eluting in the group of C_{15} and C_{16} chains (Fig. 2). Selected dimethyl-substituted isomers were analyzed after conversion into the corresponding picolinyl esters. For instance, the GC/EI-MS of the picolinyl ester of 8,11-diMe-14:0 showed M^+ at m/z 347, $[M-C_2H_5]^+$ at m/z 318, $[M-C_3H_7]^+$ at m/z 304 followed by a gap of 28 u, which prove evidence for a methyl branch on C-11. The second gap of 28 u was found between m/z 248 and m/z 220, which is in agreement with 8,11-dimethyl-14:0 (Fig. 3). In the same manner further branched-chain fatty acids could be tentatively assigned (Table 1).

3.3. Monoenoic fatty acids in vernix caseosa

Most of the monoenoic fatty acids in vernix caseosa are not available as reference standards. The presence of many different isomers made it almost impossible to determine them individually. Selected monoenoic fatty acids were studied by means of their picolinyl esters (Table 1). These measurements also verified the presence of isomers with double bonds in positions C-6 to C-10 and higher. A branched *trans*-isomer with the double bond at the lower end of the typical range which was identified due to its late elution from the RP-HPLC system (Table 1). Indications for a few further *trans*-isomers were found for the same reason. Except for these examples, the most compounds were found on the lines estimated for $\Delta 6$ – $\Delta 10$ due to known standards. However, we did not

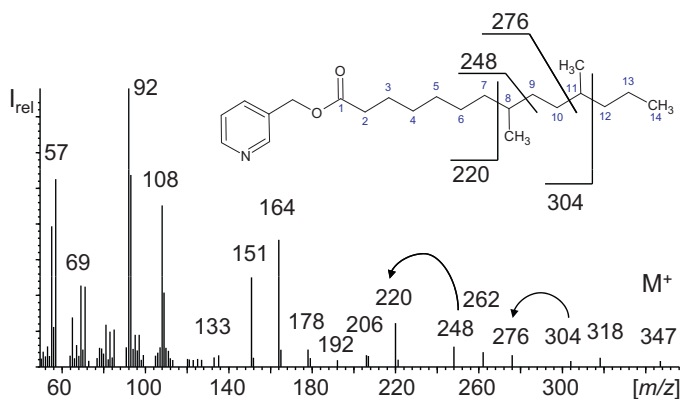


Fig. 3. GC/EI-MS spectrum of the picolinyl ester of 8,11-dimethyltetradecanoic acid (structure inserted).

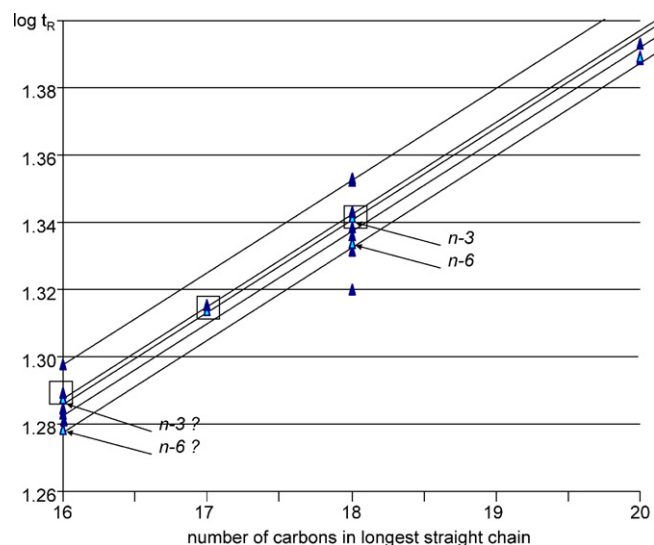


Fig. 4. Plot of logarithmic retention times ($\log t_R$) against the length of the longest carbon chain of dienoic fatty acids in vernix caseosa.

add these details to Table 1. Six isomers eluting early from the GC column were identified as branched-chain monoenoic fatty acids (Table 1). When these C_{15} – C_{18} isomers were grouped with regard to the longest chain length, the corresponding $\log t_R$ -against-longest chain plot allowed for a tentative identification of $\Delta 6$ *iso*- and $\Delta 8$ *iso*-fatty acids. Even numbered $\Delta 6$ *iso*-fatty acids were found to be dominant in vernix caseosa [4] whereas odd-numbered were not reported by these authors but by Haahti et al. [3]. The seventh branched chain monoenoic fatty acid eluted much later from the GC column which pointed either to a double bond more remote from the head group or, more likely, an unsaturated *anteiso*-fatty acid. In order to clarify this point, an aliquot of the respective fraction was hydrogenated which resulted in a higher peak for a 17:0 while i17:0 was not formed at any amount. Thus, the respective compound was an a17:1 isomer. Two monoenoic *anteiso*-fatty acids were available as standards, i.e. a17:1 $\Delta 5$ [18] and a17:1 $\Delta 12$ [35]. The a17:1 isomer detected in vernix caseosa eluted between the two reference standards and the double bond was most likely located on $\Delta 8 \pm 1$.

3.4. Dienoic and trienoic fatty acids (PUFAs) in vernix caseosa

PUFAs could be easily identified in the GC/EI-MS-SIM chromatograms by means of the higher abundance of m/z 79 relative to m/z 81 [21]. Altogether, 21 dienoic and six trienoic fatty acids were detected in the sample. The 16:2 and 18:2 contributed with seven and nine isomers to this class of fatty acids. Not a single 16:2 isomer was available as reference standard, and all detected isomers eluted into the same HPLC fraction (Table 1). Hence, it is unlikely that 16:2 isomers with one or both double bonds in *trans*-configuration were present in this sample (Table 1 and Fig. 1). No clear indication was found for branched chain 16:2 isomers. The 18:2 isomers showed a very similar picture. Plots of the $\log t_R$ against the carbon number of the longest straight chain provided similar relationships as found before for monoenoic fatty acids. Due to the similar pattern of 16:2 and 18:2 isomers starting from the last eluting isomers (uppermost line in Fig. 4). From this starting point, many of the fatty acids were grouped on straight parallel lines (Fig. 4). Two 18:2 isomers, i.e. 18:2(9,12) or 18:2n-6 and 18:2(12,15) or 18:2n-3, were available as standards. The respective lines crossed points in the 16:2 pool, and this indicated that the respective 16:2 isomers were also present in the sample (Fig. 4). Moreover, indications for 17:2n-3 and 20:2n-6 could be estimated from the plot while no evidence was found for the presence of 17:2n-6 and 20:2n-3

(Fig. 4). Noteworthy as well, the isomer following the potential 18:2*n*-3 in its GC retention time was also found in the 16:2 and 17:2 (marked with squares in Fig. 4). In addition, a late eluting 16:2 and 18:2 isomer, respectively, was detected in the sample. The main difference between 16:2 and 18:2 isomers was the early-eluting 18:2 isomer. Three of the six trienoic C₁₈ and C₂₀ fatty acid could be identified. Noteworthy, only 20:3*n*-3 but not 18:3*n*-3 was detected whereas both *n*-6 isomers were found. The other isomers could not be identified and they did not appear on straight lines in log-*t_R* against carbon length plots (data not shown).

3.5. Individual contributions to the total fatty acids in vernix caseosa

Sixteen of the 133 fatty acids contributed with more than 1% to the total fatty acids detected in vernix caseosa (Table 1). Except for two fatty acids (one 16:1 and one 18:1 isomer), all fatty acids which contributed with more than 1% to the total fatty acids in the sample could be identified (Table 1). Saturated fatty acids contributed with ~75% to the total fatty acids (46% were straight chained and ~29% branched chained), followed by monoenoic (~22%), dienoic (2.3%) and trienoic (0.2%) homologues (Table 1). The highest contribution originated from 14:0 (17%), 16:0 (13.6%), 15:0 (10.4%), and 16:1(9) (9.5%). High relative contributions were also found for *i*14:0, 4,11-diMe-14:0, and *a*15:0 which all slightly exceeded a 4% contribution to the total fatty acids. Note however that the abundances of the fatty acid are subject to natural variations and the fatty acid pattern and the concentrations presented cannot be generalized.

3.6. Enantioseparation of *anteiso*-fatty acids in vernix caseosa

The high number of methyl-branched fatty acids gave rise to the presence of many chiral fatty acids in vernix caseosa. All branched chain fatty acids except the *iso*-forms are chiral. Thus, we detected ~60 chiral fatty acids in the sample (including the monoenoic *a*17:1 isomer). These represented ~45% of all fatty acids detected in the sample. However, enantioselective studies of fatty acids in vernix caseosa had not been carried out. Without the availability of reference standards it turned out difficult to assess the enantiomeric excess of the chiral fatty acids with the exception of the *anteiso*-fatty acids. Previously, it was found that the *S*-*anteiso*-fatty acids were dominant in food [16,17]. However, in most occasions the *R*-enantiomer was detected as well. The enantioseparation of the *anteiso*-fatty acids in the sample led to surprising results (Fig. 5). While the *a*17:0 was virtually enantiopure (Fig. 5c), *a*15:0 contained significant proportions of the *R*-enantiomer (Fig. 5b). The same was also found for *a*13:0 (Fig. 5a) for which we present the first GC enantioselective data. The absence of interfering isomers was controlled by normalizing the ion traces screened in SIM-mode [16]. The SIM traces must fall together for both enantiomers in case they are not interfered (Fig. 5a–c, lower panels). Fig. 5d shows the example of an isomer which did not fulfil this condition which clarified that the peaks were interfered. We also studied the enantioselectivity of the monoenoic *anteiso*-fatty acid identified in the sample (see above). The enantioselective analysis resulted in a broad peak for the *a*17:1 isomer which indicated significant contribution of the *R*-enantiomer (Fig. 6). To provide further evidence as to the correct peak assignment, the hydrogenated fraction (which now contained the *a*17:0, see above) confirmed the presence of high proportions of the *R*-enantiomers in the sample. However, the reasons for the presence or absence of the *R*-enantiomers in the different *anteiso*-fatty acids could not be explained.

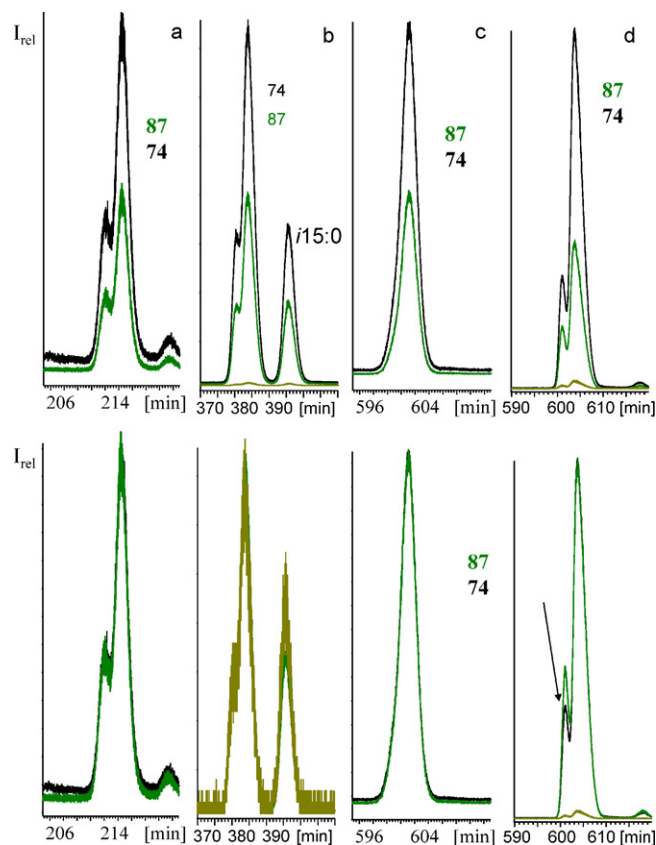


Fig. 5. GC/EI-MS-SIM gas chromatograms (black: *m/z* 74, green *m/z* 87, yellow: *M*⁺) of the enantioseparation of *anteiso*-fatty acids from vernix caseosa as methyl esters on β-TBDM. (a) *a*13:0, (b) *a*15:0 (along with the non-chiral *i*15:0), (c) *a*17:0, and an unknown 17:1 isomer. Lower panels: ion chromatograms normalized to the peaks of the *anteiso*-fatty acid. The major peak in (a)–(c) originates from the *S*-enantiomer, whereas the earlier eluting *R*-enantiomer was abundant in (a) and (b).

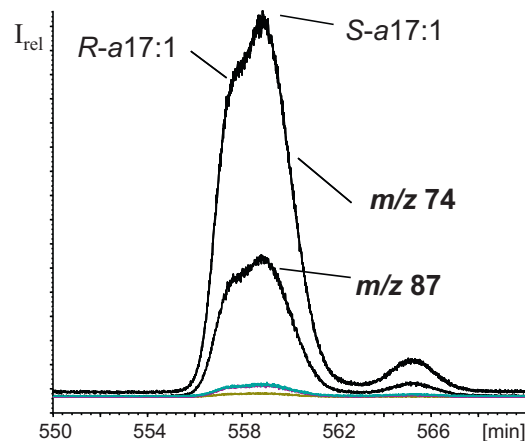


Fig. 6. GC/EI-MS-SIM gas chromatograms of the enantioseparation of *anteiso*-fatty acids from vernix caseosa as methyl esters on β-TBDM.

4. Conclusions

The fractionation of FAMES from vernix caseosa by non-aqueous HPLC followed by GC/EI-MS analysis resulted in the detection of >130 peaks. This variety in fatty acids was comparable to a fish oil sample previously analyzed [14]. However, more than half of the FAMES were only detected in one of the samples, respectively. While fish oil contained many polyenoic fatty acids not available as standard compounds, the same extend of unknowns was found

in vernix caseosa in the group of branched chain fatty acids. The 2D plot proved to be helpful in order to visualize groups of fatty acids with different number of double bonds. Thus, analysis of the HPLC fractions by GC was free of overlap by fatty acids with different number of double bonds. With this knowledge, the coordinate plots described in this study (Fig. 1b) turned out to be a valuable tool for the assessment of fatty acids in biological samples. However, due to the lack of many reference standards and the partial elution of isomers into the same fraction despite the HPLC fractionation step, structures could not be assigned to all fatty acids. Leftover-aliquots from the HPLC fractionation can be used for additional experiments of measurements. This was exemplarily done in form of hydrogenation, conversion into picolinyl esters for GC/El-MS measurements, and enantioselective analysis. Especially the results of the enantioselective analyses clarified that more research is required to elucidate the origins for the formation of *S-anteiso*-fatty acids accompanied with different proportions of R-enantiomers.

Acknowledgement

We are grateful to Holger Jost, medical doctor in Esslingen (Germany) for making the vernix caseosa sample available to us.

References

- [1] R. Rissmann, H.W.W. Groenink, A.M. Weerheim, S.B. Hoath, M. Ponec, J.A. Bouwstra, J. Invest. Dermatol. 126 (2006) 1823–1833.
- [2] P.H. Hoeger, V. Schreiner, I.A. Klaassen, C.C. Enzmann, K. Friedrichs, O. Bleck, Brit. J. Dermatol. 146 (2002) 194–201.
- [3] E. Hahti, T. Nikkari, A.M. Salmi, A.L. Laaksonen, Scand. J. Clin. Lab. Invest. 13 (1961) 70–73.
- [4] N. Nicolaides, H.C. Fu, M.N.A. Ansari, G.R. Rice, Lipids 7 (1972) 506–517.
- [5] N. Nicolaides, J.M.B. Apon, D.H. Wong, Lipids 11 (1976) 781–790.
- [6] M.E. Steward, A. Mara, B.S. Quinn, D.T. Downing, J. Invest. Dermatol. 78 (1982) 291–295.
- [7] H. Janssen, W. Boers, H. Steenberg, R. Horsten, E. Floter, J. Chromatogr. A 1000 (2003) 385–400.
- [8] L. Mondello, A.P.Q. Casilli, P.Q. Tranchida, P. Dugo, G. Dugo, J. Chromatogr. A 1019 (2003) 187–196.
- [9] S. de Koning, H.G. Janssen, M. Van Deursen, U.A.T. Brinkman, J. Sep. Sci. 27 (2004) 397–409.
- [10] T. Hyoetyläinen, M. Kallio, M. Lehtonen, S. Lintonen, P. Peraejoki, M. Jussila, M.L. Riekkola, J. Sep. Sci. 27 (2004) 459–467.
- [11] P.Q. Tranchida, P. Dugo, G. Dugo, L. Mondello, J. Chromatogr. A 1054 (2004) 3–16.
- [12] B. Vlaeminck, J. Harynuk, V. Fievez, P. Marriott, Eur. J. Lipid Sci. Technol. 109 (2007) 757–766.
- [13] S.T. Chin, Y.B.C. Man, C.P. Tan, D.M. Hashim, J. Am. Oil Chem. Soc. 86 (2009) 949–958.
- [14] S. Hauff, W. Vetter, Anal. Bioanal. Chem. 396 (2010) 2695–2707.
- [15] T. Kapp, W. Vetter, J. Chromatogr. A 1216 (2009) 8391–8937.
- [16] S. Thurnhofer, G. Hottinger, W. Vetter, Anal. Chem. 79 (2007) 4696–4701.
- [17] S. Hauff, G. Hottinger, W. Vetter, Lipids 45 (2010) 357–365.
- [18] S. Hauff, L. Rilfors, G. Hottinger, W. Vetter, J. Chromatogr. A 1217 (2010) 1683–1687.
- [19] S. Thurnhofer, K. Lehnert, W. Vetter, Eur. Food Res. Technol. 226 (2008) 975–983.
- [20] S. Hauff, W. Vetter, J. Agric. Food Chem. 57 (2009) 3423–3430.
- [21] S. Thurnhofer, W. Vetter, J. Agric. Food Chem. 53 (2005) 8896–8903.
- [22] W. Vetter, M. Schröder, Food Chem. 119 (2010) 746–752.
- [23] J.M.B. Apon, N. Nicolaides, J. Chromatogr. Sci. 13 (1975) 467–473.
- [24] N. Nicolaides, Lipids 6 (1971) 901–905.
- [25] A. Dietrich, B. Maas, W. Messer, G. Bruche, V. Karl, A. Kaunzinger, A. Mosandl, J. High Resolut. Chromatogr. 15 (1992) 590–593.
- [26] R.L. Glass, T.P. Krick, D.M. Sand, C.H. Rahn, H. Schlenk, Lipids 10 (1975) 695–702.
- [27] O. Bertelsen, N. Dinh-Nguyen, Fette Seifen Anstrichm. 87 (1985) 336–342.
- [28] F. Destailats, P. Angers, J. Am. Oil Chem. Soc. 79 (2002) 253–256.
- [29] W. Vetter, I. Wegner, Chromatographia 70 (2009) 157–164.
- [30] M.P. Mansour, J. Chromatogr. A 1097 (2005) 54–58.
- [31] J.T. Lin, T.A. McKeon, A.E. Stafford, J. Chromatogr. A 699 (1995) 85–91.
- [32] E. Bravi, G. Perretti, L. Montanari, J. Chromatogr. A 1134 (2006) 210–214.
- [33] R.R. Ran-Ressler, S. Devapatla, P. Lawrence, J.T. Brenna, Pediat. Res. 64 (2008) 605–609.
- [34] F.P. Woodford, C.M. van Gent, J. Lipid Res. 1 (1960) 188–190.
- [35] S. Thurnhofer, W. Vetter, Tetrahedron 63 (2007) 1140–1145.